S E S 2 0 1 1
Seventh Scientific Conference with International Participation
SPACE, ECOLOGY, SAFETY
29 November – 1 December 2011, Sofia, Bulgaria

PROFILE OF THE SPACE RADIATION BETWEEN EARTH SURFACE AND MOON ORBIT

Tsvetan Dachev

Space Research and Technology Institute – Bulgarian Academy of Sciences
e-mail: tdachev@bas.bg

Keywords: *Space radiation, Space weather, Dosimetry, Spectrometry*

Abstract: *Since 2000 scientists from Space and Solar-Terrestrial Research Institute at the Bulgarian Academy of Sciences contributed with Bulgarian build instruments in number of experiments for measurements of the incoming space radiation fluxes and dose rates from Earth Surface to the Moon Orbit. This paper summarizes the results obtained by different instruments on the ground and in aircraft, balloon, rocket, and on Earth, and Moon spacecraft. Data from these experiments are analyzed, compared and plotted to reveal harmonized picture how the different ionizing radiation sources contribute and build the space radiation altitudinal profile from the earth surface to the moon orbit.*

ПРОФИЛ НА КОСМИЧЕСКАТА РАДИАЦИЯ МЕЖДУ ЗЕМНАТА ПОВЪРХНОСТ И ОКОЛОЛУННА ОРБИТА

Цветан Дачев

Институт за космически изследвания и технологии – Българска академия на науките
e-mail: tdachev@bas.bg

Ключови думи: *Космическа радиация, Космическо време, Дозиметрия, Спектрометрия*

Абстракт: *Учените от Института за космически и слънчево-земни изследвания на Българската академия на науките след 2000 г. участваха с български прибори в серия от експерименти за измерване на дозата и потока космическа радиация от повърхността на Земята до окололунна орбита. Тази статия сумира резултатите получени с различни прибори, както на земната повърхност и в атмосферата със самолети, балони и на спътници на Земята и Луната. Получените от тези експерименти данни са анализирани, сравнени и представени като единен, синтезиран, високочинен профил на разпределението на дозата и потока космическа радиация от земната повърхност до окололунна орбита.*

1. Introduction

The radiation field around the ISS is complex, composed by galactic cosmic rays (GCR), trapped radiation of the Earth radiation belts, solar energetic particles, albedo particles from Earth's atmosphere and secondary radiation produced in the shielding materials of the spacecraft and in biological objects.

1.1. Galactic cosmic rays

The dominant radiation component in near Earth and Moon space environment are the galactic cosmic rays (GCR) modulated by the solar activity. The GCR are charged particles that originate from sources beyond our solar system. They are thought be accelerated at the highly energetic sources like neutron star, black holes and supernovae within our Galaxy. GCR are the most penetrating of the major types of ionizing radiation. The distribution of GCR is believed to be isotropic throughout interstellar space. The energies of GCR particles range from several tens up to 10^{12} MeV nucleon^{-1}. The GCR spectrum consists of 98% protons and heavier ions (baryon component) and 2% electrons and positrons (lepton component). The baryon component is composed of 87% protons, 12% helium ions (alpha particles) and 1% heavy ions (Simpson, 1983). Highly energetic particles in

the heavy ion component, typically referred to as high Z and energy (HZE) particles, play a particularly important role in space dosimetry (Benton and Benton, 2001). HZE particles, especially iron, possess high-LET and are highly penetrating, giving them a large potential for radiobiological damage (Kim et al., 2010). Up to 1 GeV, the flux and spectra of GCR particles are strongly influenced by the solar activity and hence shows modulation which is anti-correlated with solar activity.

1.2. Trapped radiation belts

Radiation belts are the regions of high concentration of the energetic electrons and protons trapped within the Earth's magnetosphere. There are two distinct belts of toroidal shape surrounding Earth where the high energy charged particles get trapped in the Earth's magnetic field. Energetic ions and electrons within the Earth's radiation belts pose a hazard to both astronauts and spacecraft. The inner radiation belt, located between about 0.1 to 2 Earth radii, consists of both electrons with energies up to 10 MeV and protons with energies up to ~ 100 MeV. The outer radiation belt (ORB) starts from about 4 Earth radii and extends to about 9-10 Earth radii in the anti-sun direction. The outer belt mostly consists of electrons whose energy is not larger than 10 MeV. The electron flux may cause problems for components located outside a spacecraft (e.g. solar cell degradation). They do not have enough energy to penetrate a heavily shielded spacecraft such as the ISS wall, but may deliver large additional doses to astronauts during extra vehicular activity (Dachev et al., 2009). The main absorbed dose inside the ISS is contributed by the protons of the inner radiation belt. The South-Atlantic Anomaly (SAA) is an area where the radiation belt comes closer to the Earth surface owing to a displacement of the magnetic dipole axes from the Earth's center. The daily average SAA doses reported by Reitz et al.(2005) inside of the ISS vary in the range 74-215 μGy d^{-1} for the absorbed dose rates and in the range 130-258 μSv d^{-1} for the averaged equivalent daily dose rates.

1.3. Solar Energetic Particles (SEP)

The SEP are mainly produced by solar flares, sudden sporadic eruptions of the chromosphere of the Sun. High fluxes of charged particles (mostly protons, some electrons and helium and heavier ions) with energies up to several GeV are emitted by processes of acceleration outside the Sun. The time profile of a typical SEP starts off with a rapid exponential increase in flux, reaching a peak in minutes to hours. The energy emitted lies between 15 and 500 MeV $nucleon^{-1}$ and the intensity can reach 104 cm^{-2} s^{-1} sr^{-1}. Electrons with energies of ~0.5 to 1 MeV arrive at Moon, usually traveling along interplanetary field lines, within tens of minutes to tens of hours. Protons with energies of 20 to 80 MeV arrive within a few to ~10 hours, although some high energy protons can arrive in as little as 20 minutes. SEP are relatively rare and occur most often during the solar maximum phase of the 11-year solar cycle. In the years of maximum solar activity up to 10 flares can occur, during the years of minimum solar activity only one event can be observed on average (Lantos, 1993).

1.4. Lunar albedo radiation

The lunar albedo radiation (principally neutrons) (De Angelis et al., 2005) is produced by the interactions of GCRs and SEPs in the surface. The neutron albedo can contribute as much as ~20% to the effective dose when the radiation environment is dominated by GCRs, whereas when SEPs dominate, the neutrons contribute ~2% to the effective dose (Kim et al., 2010).

2. Instruments description

The main purpose of Liulin type Deposited Energy Spectrometer (DES) is to measure the spectrum (in 256 channels) of the deposited energy in the silicon detector from primary and secondary particles at the aircraft altitudes, at Low Earth Orbits (LEO), outside of the Earth magnetosphere on the route and on the surface of the planets of Solar system. The DES is a Liulin type (Dachev et al. 2002) miniature spectrometer-dosimeter containing: one semiconductor detector, one charge-sensitive preamplifier, 2 or more microcontrollers and a flash memory. Pulse analysis technique is used for the obtaining of the deposited energy spectrum, which further is used for the calculation of the absorbed dose and flux in the silicon detector. The unit is managed by the microcontrollers through specially developed firmware. Plug-in links provide the transmission of the stored on the flash memory data toward the standard Personal Computer (PC) or toward the telemetry system of the carrier. DES sensitivity was proved against neutrons and gamma radiation (Spurny and Dachev, 2002, 2009), which allows monitoring of the natural background radiation also.

For the analysis of altitudinal profile of the space radiation since 2000 following Liulin type spectrometers were used in near Earth and Moon radiation environment on different carriers:

- Liulin-MDU1 launched on 14th of June 2000 at ESA balloon flight up to 29 km over the Gap town, France;

- Mobile Dosimetry Unit MDU#1 of Liulin-4U instrunent was used on the Deep Space Test Bed (DSTB) during the 8 June 2005 certification flight from Ft. Sumner, New Mexico up to 37.3 km altitude (Benton, 2005). It was a part of the NASA Space Radiation Shielding Program, Marshall Space Flight Center;
- Mobile Dosimetry Unit MDU-5 was used between 5th of June and 29th of July 2005 on aircraft of Czech Airlines (CSA) at different routes. The experiments and data analysis were managed by Prof. F. Spurny (Spurny and Dachev, 2009);
- Radiation Risks Radiometer-Dosimeter (R3D) for Biopan (R3D-B) with 256 channels ionizing radiation monitoring spectrometer and 4 channels UV spectrometer known as R3D-B2 was successfully flown 31 May – 16 June 2005 inside of the ESA Biopan 5 facilities on Foton M2 satellite. The operation time of the instrument was about 20 days for fulfilling of the total 1.0 MB flash memory with 60 sec resolution (Häder et al., 2009);
- RADOM instrument was launched successfully on Indian Chandrayaan-1 satellite on 22nd of October 2008. It starts working 2 hours after the launch with 10 seconds resolution behind about 0.45 g.cm^{-2} shielding. The instrument sends data for number of crossings of the Earth radiation belts and continues to work on 100 and 200 km circular lunar orbit measuring mainly the GCR environment (Dachev et al., 2009, 2011).

3. Scientific results

3.1. Example for the space radiation distribution from Earth to orbit of Foton M2 satellite

The doses of ionizing radiation were measured continuously from 24 May to 12 June 2005 on Foton M2 satellite with the R3D-B2 instrument (Häder et al., 2009). Figure 1 shows three important periods recorded at 1-min resolution in the time interval 25 May-3 June 2005. Moving averages curves over 30 points for dose rate (heavy dashed line) and dose to flux ratio were plotted on the figure. The lowest doses in the left part of the figure were obtained after 16:00 UT on 24 of May 2005 when the mounting of R3D-B2 into the Biopan 5 facility occurred. These few different values obtained in Nederland, Russia and Kazakhstan of about 0.08 μGy h^{-1} are comparable with the natural background radiation with a world mean value about 0.0585 μGy h^{-1} (Ghiassi-nejad, 2002). Two maxima occur during the two aircraft flights from Amsterdam to Samara, Russia and from Samara to Baikonur. The highest dose rate values obtained during the flights were about 3.2 μGy h^{-1} for the first flight and 2.3 μGy h^{-1} for the second flight. The difference is produced most probably by different altitudes of the flights.

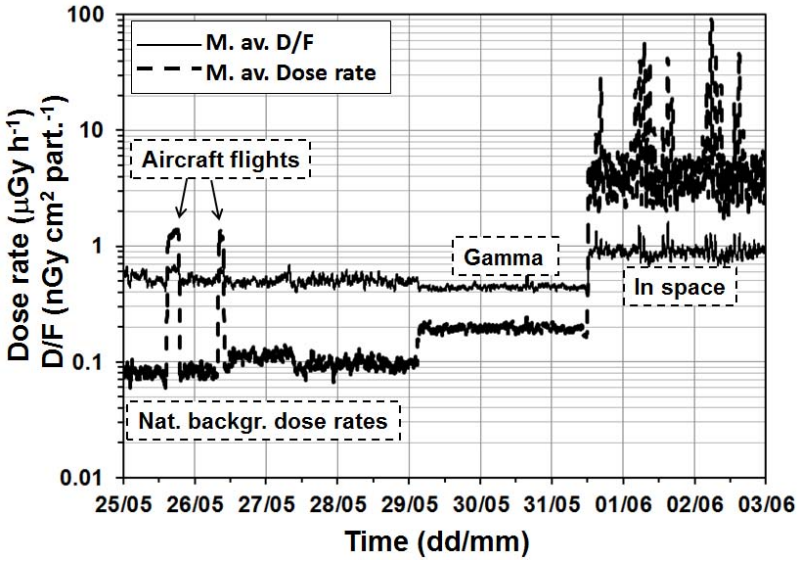

Fig. 1. Variations of the average deposited dose rate for transatlantic flights at altitude 10.6 km.

The doses in the central part of the figure are obtained after the integration of the Biopan 5 facility on the Foton M2 satellite. The increase of the doses up to 0.196 μGy h^{-1} in this part of the recording is the result of additional radiation produced by a gamma ray source on the Foton M2 capsule used for the determination of automatic rocket fire before the touchdown of the capsule. Right side data are from the flight of the satellite in orbit.

The recorded maxima in the right side part of Figure 1 are obtained in space during the crossing of the South-Atlantics magnetic anomaly (SAA) region where the inner radiation belt populated with high-energy protons is encountered and from the outer radiation belt populated by relativistic electrons (Dachev et al., 2009).

The values of the dose rate to flux curve (D/F) gives some information of the type of predominant radiation sources measured by the instrument This methodology is based on the experimental formulas published by Heffner (Heffner, 1971) and recently described for the Liulin type dosimeters (Dachev, 2009). The experimental formulas (Heffner, 1971) shows that protons in the range 10-300 MeV as in the inner radiation belt can delivery specific doses per particle always above

1 nGy cm^{-2} particle^{-1}, while the specific doses by electrons in the range 1-10 MeV are less than 1 nGy cm^{-2} particle^{-1}. Same is truth for muons and all kind of electromagnetic radiation as roentgen and gamma. It is seen that the D/F value in left part of the figure is stable with values around 0.5 nGy cm^{-2} particle^{-1}. These low values are indicator of small energy depositing events in the instrument which are generated mainly by muons and gamma rays. The D/F values fall down to about 0.42 nGy cm^{-2} particle^{-1} when the doses start to be built by gamma radiation source on the board of the capsule.

After the launch on 31st of May about noon the D/F mean values increase and stay at about 0.9 nGy cm^{-2} particle^{-1} in most of the time in orbit. These values are interpreted as caused by the GCR particles (Dachev, 2009). Crossings of the regions of SAA increase these values above 1 nGy cm^{-2} particle^{-1}, where protons are predominating and decrease below it during the crossings of the other radiation belt regions populated mainly by relativistic electrons. This behavior is repeatedly seen on 2nd and 3rd of June when before and after noon SAA crossings occur and inner belt crossings are about 10-11 hour in the morning.

The conclusion from this section of the paper is that in the simplest case with same instrument in all around Earth radiation sources.

3.2 Altitudinal profile of the space radiation between earth surface and moon orbit

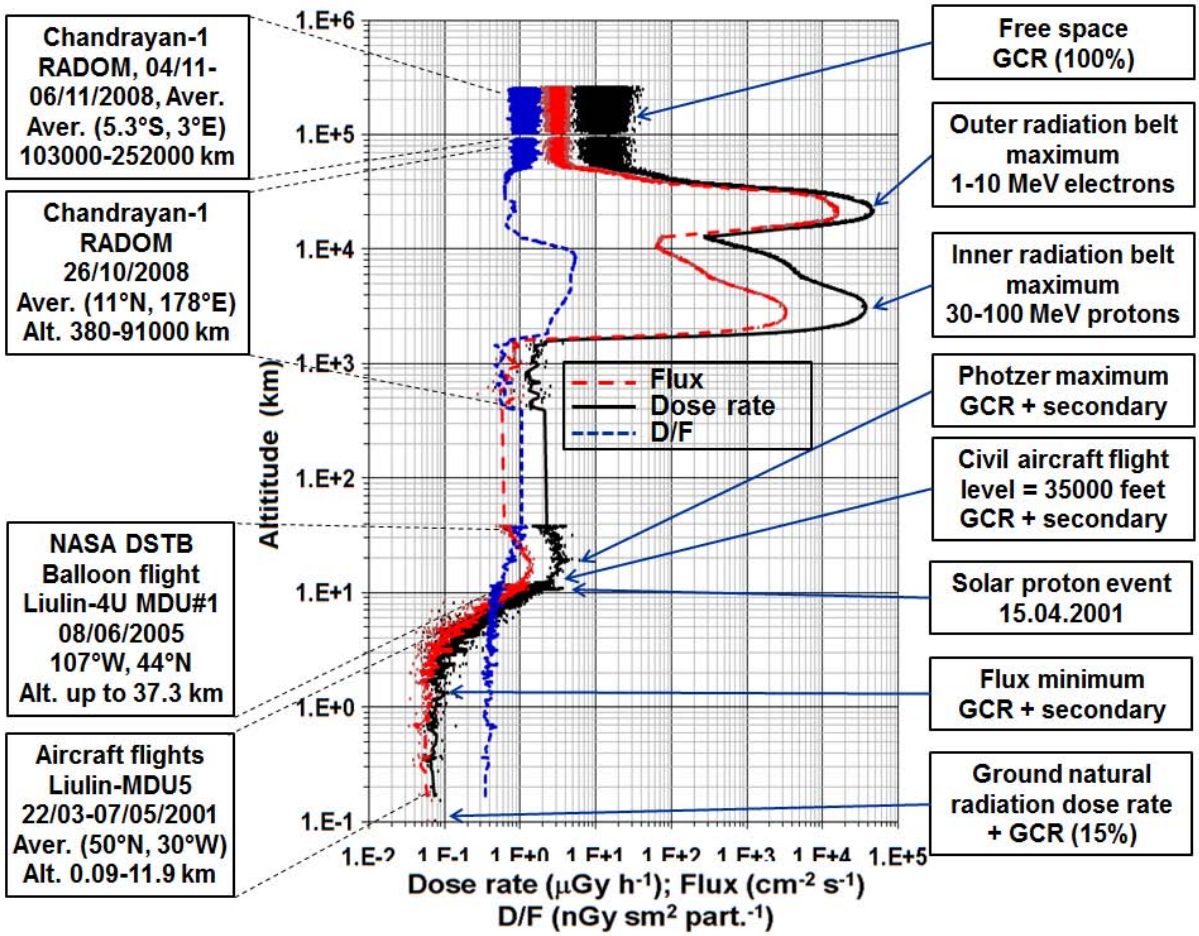

Fig. 2. Variations of the absorbed dose rate flux and dose to flux for synthetic altitudinal profile from 0.1 to more than 250000 km.

Figure 2 presents the synthesized altitudinal profiles of the moving averages (over 4 points) of 3 parameters: absorbed dose rate in μGy h^{-1} (heavy line), flux in cm^{-2} s^{-1} (long dashed line) and dose rate to flux ratio in nGy cm^{-2} particle^{-1} (short dashed line). In the left side of the figure are listed the carriers, instruments, time, averaged geographic coordinates of the measured values and their altitudinal range in km. On the right side are listed the conditions and predominant radiation sources for the places pointed with the strikes.

3.2.1. Ground natural radiation dose rate

The lowest point in Figure 2 represents the values of the mentioned above 3 parameters obtained by averaging of 2431 points with 10 minutes resolution obtained during the measurements in the airports at altitude above the see level (a.s.l.) between zero and 500 meters, which we accept as

average value of 100 m a.s.l. The exact average value is 0.073 μGy h^{-1}. Other parameters values and their ranges are given in Table 1. Different airports shows different dose rate mean values being maximal in Prague airport - D=0.075 μGy h^{-1} and minimal in the Dubai airport D=0.058 μGy h^{-1}. These values are in good agreement with the world average natural background radiation dose rate, which is 0.0585 μGy h^{-1} (Ghiassi-nejad et al., 2002) with minimum dose rate of 0.018 and maximum of 0.095 μGy h^{-1}.

Table 1. Averaged data concerning points of interest on Fig. 2.

Point description, number of the measurements used, time [dd/mm/yyyy]	**Averaged altitude, range [km]**	**Averaged geographic coordinates [long, lat]**	**Averaged dose rate and range [μGy h^{-1}]**	**Averaged flux and range [cm^{-2} s^{-1}]**	**Averaged D/F and range [nGy cm^{-2} $particle^{-1}$]**
Ground, 2431, 22/03-07/05/2001	0.1	2°W, 48°N	0.073 0.026-0.212	0.059 0.0028-0.111	0.346 0.213-1.15
Flux minimum, 10, 22/03-04/05/2001	1.6 1.56-1.7	51°W, 45°N	0.073 0.049-0.114	0.052 0.04-0.072	0.386 0.325-0645
Civil aircraft flight level between 34000 and 36000 feet (10.668 km), 559 points, 22/03/2001-05/05/2001	10.5457 10.3632-10.668	31°W, 52°N	1.62 0.85-2.33	0.921 0.534-1.068	0.4881 0.4032-0.6365
Photzer maximum GCR + secondary, 2, 08/06/2005	19 (dose) 16.4-29.1 15 (flux) 12-21	107°W, 44°N	3.2	 1.54	0.6 0.56
Inner radiation belt maximum 30-100 MeV protons, 2 26/10/2008 01:58:15	3007 2984-3031	165°E,15.3°S	37280	3127	3.31
Outer radiation belt maximum 1-10 MeV electrons, 6 26/10/2008 03:03:04	21386	149°W,15.8°S	46335	14473	0.89
Free space GCR (100%), 8314	229000 200000-251000		12.77	3.16	1.13

3.2.2. Flux minimum at 1.6 km altitude

Next interesting point on Figure 1 was the flux minimum observed at altitudes around 1.6 km. This is the point where the terrestrial component of the background radiation can be neglected but the cosmic radiation component is still at very low levels. The observed by us averaged value of the altitude of 1.6 km which was equal to the calculated value by the GEANT-4 model (Bazilevskaya et al., 2009). Our flux value was 0.052 cm^{-2} s^{-1}, while the predicted by the GEANT-4 model is 0.025 cm^{-2} s^{-1}. From other hand the measured average value for 1976 by (Bazilevskaya et al., 2009) is 0.052 cm^{-2} s^{-1}. The dose rate at these altitudes observed by us also shows some time well seen minimum as published on figure 10 of (Dachev et al., 2002) but in the case of Figure 1 it is not well formed. Exact values for this point and their ranges are seen at Table 1.

3.2.3. Civil aircraft flight level at 35000 feet

At altitudes above the point of minimal flux the dose rate and flux start to increase rapidly because of the domination of the cosmic radiation component. We obtain polynomial fitting approximations by factor of 2 of the dose rate and flux in dependence of altitude:

(1) Flux[cm^{-2} s^{-1}]Dose rate[μGy h^{-1}]=0.0111*alt^2[km]-0.0369*alt[km]+0.0774

(2) Dose rate[μGy h^{-1}]= 0.0221*alt^2[km]-0.00951*alt[km]+0.01579

where “alt” is the altitude in km.

As seen in Figure 2 the plotting of the dose rate and flux in the altitudinal range 0.1-12 km gives strong variations of the measured values. The R-squared value for the flux is R^2=0.9115, while for the dose rate the obtained during process of polynomial approximation is R^2=0.8301, which is relatively low value. The average values of dose rate and flux at flight levels between 34000 and 36000 feet) (10.668 km) is obtained to be Dose=1.62 μGy h^{-1} and Flux=0.921 cm^{-2} s^{-1} by averaging of 559 measurements in the time interval 22/03/2001-05/05/2001. The ranges for the values of the dose rate is as seen from Table 1 between 0.85 and 2.33 μGy h^{-1}. The reason is that large amount of data are obtained at standard nominal altitudes, measured in thousands of feet at different latitudes and longitudes.

3.2.4. Geographic map of dose rate at flight level at 35000 feet

Figure 3 aims to answer the question how the large ranges in the values of dose rate are distributed in latitudes and longitudes for a period between 6th of May and 28th of June 2002. Data obtained mainly during flights from Prague to New York and Montreal and back are used. Some amount of data covers the east low latitudes by flights from Prague to Dubai and back. The Prague airport is on the following coordinates: Latitude=50.15°N,Longitude=14.37° E, Altitude=1123 m above the sea level. The dose rate data obtained at standard nominal altitude of 35000 feet (10.67 km) are plotted in the figure in dependence of the geographic latitude and longitude.

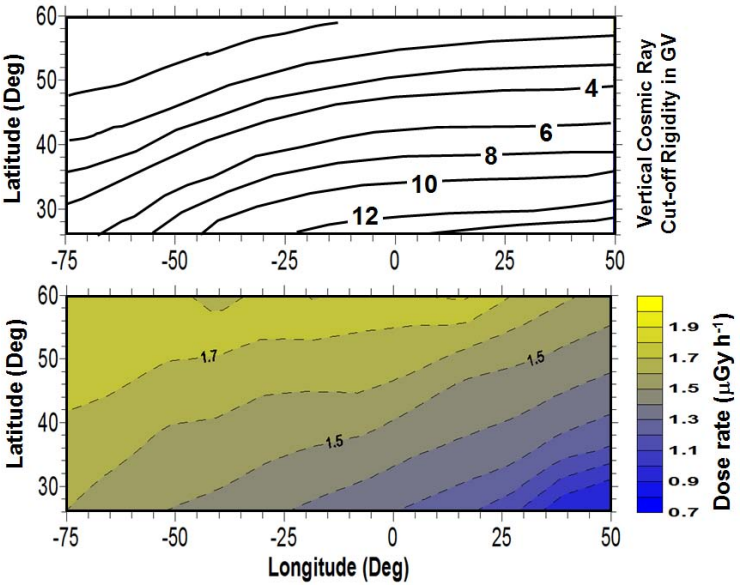

Fig. 3. 2D variations of the absorbed dose rate for region in Northern hemisphere between 75°W and 50°E longitude at altitude around 35000 feet (10.67 km).

The grid was obtained from 1043 measurements by the method of minimum curvature, which was with 5° and 10° spacing in latitude and longitude respectively. The linear gray level scale in the left side of the figure is with minimal and maximal values of 0.7 and 2.1 μGy h^{-1}. It is well seen that the minimum dose rate values are obtained at low latitudes in the longitudinal range 25°-50° East longitude. The maximum dose rates are in the high latitudes in the longitudinal range 25°W-75°W. The reason for this distribution is seen in the upper panel of Figure 2 where the vertical cosmic ray cut-off rigidity at 20 km altitude for the geomagnetic conditions in 1990 in GV is plotted (Shea and Smart, 2001). As expected following the shape of geomagnetic field lines the cut-off rigidity has its maximal values where the dose rates has minimums and in reverse at the places with minimal rigidity the maximal dose rates are observed. The higher cut-off rigidity means that the particles from the GCR and their secondary have to have higher energy to penetrate to the atmosphere. That is why at the areas with low cut-off rigidity larger flux and respectively larger dose rate is observed.

3.2.5. Photzer maximum

The interaction of the primary cosmic radiation with the atoms and molecules of the atmosphere produces a broad spectrum of different secondary particles with varying energy and linear energy transfer (LET): protons, neutrons, electrons, muons, pions, gamma-quanta and bremsstrahlung. With increasing depth in the atmosphere, the primary cosmic radiation component decreases, whereas the secondary radiation component increases. This complex situation results in a maximum of the dose rate at an altitude of 18 to 25 km where the zone of the so called Pfotzer maximum exists.

On Figure 3 it is seen that at the altitudes around 19 km the dose rate reach local maximums. These data were obtained with a Liulin battery operated MDU during the 8 June 2005 certification flight of the NASA Deep Space Test Bed (DSTB) balloon at Ft. Sumner (34.47°N 104.24°W), New Mexico, USA (Benton, 2007; Adams et al., 2007). Because the relatively lower latitude (34.47°N) the observed fluxes in the Pfotzer maximum is about 1.5-1.6 cm^{-2} s^{-1}, which value is smaller the presented by (Stozhkov et al., 2011).

3.2.6. Inner radiation belt maximum

As seen in Figure 2 upper than Photzer maximum the dose rates and fluxes decreased and stay at almost fixed levels up to the bottom side of the inner radiation belt (IRB) maximum at about 1700 km altitude. This behavior was adequate for the RADOM instrument measurements at the Indian Chandrayaan-1 satellite in October 2008 at low latitudes (Dachev et al., 2011). Measurements on the HotPay2 rocket from Andoya Rocket Range (69.29°N, 16.03°E), Norway in January 2008 (Tomov et al., 2008) shows much higher dose rates and fluxes even at 300 km altitude because larger Earth magnetic field latitude and respectively lower geomagnetic cutoff rigidity (Shea and Smart, 2001), which allowed larger GCR fluxes.

Starting from about 1700 km altitude the dose rates and fluxes increased sharply by more than 4 orders on magnitude and reached the maximums at the position of the IRB maximum at about 3000 km altitude. The major radiation source in the lower part of the IRB was high energy protons (Dachev et al., 2011). At altitudes above the IRB maximum the dose rates and fluxes decrease and reach

minimum values at about 11000 km altitude in the slot region. The D/F values raised inside of the IRB and reached values of about 5 nGy cm^{-2} $particle^{-1}$ at 9000 km altitude which correspond to energies of about 25 MeV (Heffner, 1971, Dachev, 2009).

3.2.7. Outer radiation belt maximum

Up than the slot region at 11000 km altitude the dose rates and fluxes raised again to reach new maximum in the region of outer radiation belt (ORB) maximum. Figure 2 shows that the ORB starts from ~14000 km and extends up to ~54000 km. Maximum particle flux in the outer belt were observed at ~22500 km. This maximum was populated mainly by 1-10 MeV electrons and it was confirmed by the values of the D/F ratio, which was below 5 nGy cm^{-2} $particle^{-1}$ inside of the ORB. The comparison of our RADOM ORB flux data with the predicted by the models AE-8MIN and CRESS/ELE/PRO (SPENVIS (http://www.spenvis.oma.be/) shows relatively large discrepancies. The differences between the observed data and the models data can be explained by the fact that the RADOM observations are made in relatively very low solar activity and quiet geomagnetic conditions, which was never observed before (Dachev et al., 2011).

3.2.8. Free space

The average dose rate from 8314 measurements in the altitudinal range between 200000 and 251000 km from the Earth was ~12.77 μGy h^{-1}. The range of the real measured dose rates is between 3.34 and 41.34 μGy h^{-1} with a standard deviation of 4.25 μGy h^{-1}. The average flux is 3.16 particles cm-2 cm^{-2} s^{-1}, while the real flux range is between 1.71 and 4.82 particles cm^{-2} s^{-1} with a standard deviation of 0.41 cm^{-2} s^{-1}. These values of the dose rate and flux may be used as referee values for the “free space” radiation conditions at this very low level of solar activity.

3. Summary

The paper analyzed the obtained results in the different radiation environments of Galactic Cosmic Rays at aircraft and balloon altitudes, inner radiation belt trapped protons, outer radiation belt relativistic electrons and in free space during different missions performed with Bulgarian build instruments. *Data from these experiments are compared and plotted to reveal harmonized picture how the different ionizing radiation sources contribute and build the space radiation altitudinal profile from the earth surface to the free space close to moon orbit.*

4. Acknowledgements

The author would like to thank to: B. Tomov, P. Dimitrov and Y. Matviichuk from Space Research & Technology Institute at the Bulgarian Academy of Sciences for the cooperation in the development of the Liulin type spectrometers and for the assistance with data analysis; F. Spurny, and O. Ploc from Nuclear Physics Institute, Czech Republic for the aircraft data and work on the interpretation procedure; ISRO staff and more specially to: Mr. M. Annadurai, Project Director and J. N. Goswami, Project scientist of Chandrayaan-1 satellite, P. Sreekumar and V. Sharan, Space Astronomy & Instrument Div., and Dr. J D Rao, ISTRAC/ISRO Bangalore for the RADOM instrument support. This work is partially supported by the Bulgarian Academy of Sciences and contract DID 02/8 with Bulgarian Science Fund.

References:

1. Adams, J.H., L. Adcock, J. Apple, M. Christl, W. Cleveand, M. Cox, K. Dietz, C. Ferguson, W. Fountain, B. Ghita, E. Kuznetsov, M. Milton, J. Myers, S. O’Brien, J. Seaquist, E. A. Smith, G. Smith, L. Warden and J. Watts, Nuclear Instruments and Methods in Physics Research Section A: Accelerators, Spectrometers, Detectors and Associated Equipment, Volume 579, Issue 1, 21, 522-525, August 2007.
2. Bazilevskaya, G.A., V.S. Makhmutov, Y.I. Stozhkov, A.K. Svirzhevskaya, N.S. Svirzhevsky, I.G. Usoskin, G.A. Kovaltsov and T. Sloan, Dynamics of the ionizing particle fluxes in the Earth’s atmosphere, Proceedings of the 31st ICRC, Lodz, 2009. http://icrc2009.uni.lodz.pl/proc/pdf/icrc0228.pdf
3. Benton, E.R., Benton E.V., Space radiation dosimetry in low-Earth orbit and beyond. *Nucl Instrum Methods Phys Res B*., 184(1-2), 255-294, 2001.
4. Benton, E., Deep Space ICCHIBAN: An International Comparison of Space Radiation Dosimeters aboard the NASA Deep Space Test Bed, 10th Workshop for Radiation Monitoring on ISS, Chiba, Japan, 7-9 September 2005. http://www.oma.be/WRMISS/workshops/tenth/pdf/08_benton.pdf
5. Dachev, Ts., Tomov, B., Matviichuk, Yu., Dimitrov Pl., Lemaire, J., Gregoire, Gh., Cyamukungu, M., Schmitz, H., Fujitaka, K., Uchihori, Y., Kitamura, H., Reitz,

G., Beaujean, R., Petrov, V., Shurshakov V., Benghin, V., Spurny, F. Calibration results obtained with Liulin-4 type dosimeters, Adv. Space Res. 30, 917-925, 2002. doi:10.1016/S0273-1177(02)00411-8
6. Dachev, Ts.P., B.T. Tomov, Yu.N. Matviichuk, P.G. Dimitrov, N.G. Bankov, Relativistic Electrons High Doses at International Space Station and Foton M2/M3 Satellites, Adv. Space Res., 1433-1440, 2009. doi:10.1016/j.asr.2009.09.023
7. Dachev, Ts. P., B. T. Tomov, Yu.N. Matviichuk, Pl .G. Dimitrov, F. Spurny, Monitoring Lunar radiation environment: RADOM instrument on Chandrayaan-1, Current Science, 96, 4, 544-546, 2009. ISSN: 0011-3891, 2009.
8. Dachev, Ts.P., Characterization of near Earth radiation environment by Liulin type instruments, Adv. Space Res., 1441-1449, 2009. doi:10.1016/j.asr.2009.08.007
9. Dachev, Ts. P., B. T. Tomov, Yu.N. Matviichuk, Pl .G. Dimitrov, Vadawale, S. V., J. N. Goswami, V. Girish, G. de Angelis, An overview of RADOM results for Earth and Moon Radiation Environment on Chandrayyan-1 Satellite, Adv. Space Res., 48, 5, 779-791, 2011. doi: 10.1016/j.asr.2011.05.009
10. De Angelis, G., F.F. Badavi, J.M. Clem, S.R. Blattnig, M.S. Clowdsley, J.E. Nealy, R.K. Tripathi, J.W. Wilson, A Time Dependent Model for the Lunar Radiation Environment, Paper SAE2005-01-2831, pp. 1-11, Society of Automotive Engineering (SAE), Inc., 2005.
11. Häder, D.P., P. Richter, M. Schuster, Ts. Dachev, B. Tomov, Pl. Georgiev, Yu. Matviichuk, R3D-B2 - Measurement of ionizing and solar radiation in open space in the BIOPAN 5 facility outside the FOTON M2 satellite, Adv. Space Res. Volume 43, Issue 8, Pages 1200-1211, 2009. doi:10.1016/j.asr.2009.01.021
12. Heffner, J., Nuclear radiation and safety in space, M, Atomizdat, pp 115, 1971. (in Russian).
13. Friedberg, W., K. Copeland, Ionizing Radiation in Earth's Atmosphere and in Space Near Earth, Technical Report No. DOT/FAA/AM-11/9, FAA Civil Aerospace Medical Institute P.O. Box 25082, Oklahoma City, OK 73125, May 2011. *http://www.dtic.mil/cgi-bin/GetTRDoc?Location=U2&doc=GetTRDoc.pdf&AD=ADA546541*
14. Ghiassi-nejad, M., S. M. J. Mortazavi, J. R. Cameron, A. Niroomand-rad,_ and P. A. Karam, Very High Background Radiation Areas of Ramsar, Iran: Preliminary Biological Studies, Health Physics, V 82, 1, 87-93, 2002. http://www.probeinternational.org/Ramsar.pdf
15. Kim, M.-H.Y., G. De Angelis, F.A. Cucinotta, Probabilistic assessment of radiation risk for astronauts in space missions, Acta Astronautica, Volume 68, Issues 7-8, April-May 2011, Pages 747-759, 2010.
16. Lantos, P., The Sun and its effects on the terrestrial environment. Radiat Prod Dosim. 48(1), 27-32, 1993.
17. Regener, E. & G. Pfotzer, Vertical Intensity of Cosmic Rays by Threefold Coincidences in the Stratospher, Nature 136, 718-719, 1935. doi:10.1038/136718a0
18. Reitz, G., R. Beaujean, E. Benton, S. Burmeister, T. Dachev, S. Deme, M. Luszik-Bhadra, P. Olko, Space radiation measurements on-board ISS-The DOSMAP experiment, Radiat. Prot. Dosim. 116 (1-4), 374-379, 2005.
19. Shea, M.A., Smart D.F, *Vertical Cutoff Rigidities for Cosmic Ray Stations Since 1955*, 27th International Cosmic Ray Conference, Contributed Papers, 10, 4063-4066, 2001.
20. Simpson, J.A., in: Shapiro M.M. (Ed.), Composition and origin of cosmic rays, *NATO ASI Series C: Mathematical and Physical Sciences.* Vol. 107, Reidel, Dordrecht, 1983.
21. Spurny, F., Ts. Dachev, B. Tomov, Yu. Matviichuk, Pl. Dimitrov, K. Fujitaka, Y. Uchihori, H. Kitamura, Dosimetry Measurements During a Balloon and Aircraft Flights, Proceedings of 7th STIL-BAS conference, 169, Sofia, November, 2000.
22. Spurny, F., Ts. Dachev, B. Tomov, Yu. Matviichuk, Pl. Dimitrov, K. Fujitaka, Y. Uchihori, H. Kitamura, Dosimetry Measurements During a Balloon and Aircraft Flights, Proceedings of 7th STIL-BAS conference, 169-172, Sofia, November, 2000. http://www.stil.bas.bg/a_online/balloon.htm
23. Spurny, F., T. Dachev, On Board Aircrew Dosimetry with a Semiconductor Spectrometer, Radiat. Prot. Dosim. 100, pp 525-528, 2002.
24. Spurny, F., and T.P. Dachev, New results on radiation effects on human health, Acta geophysica, vol. 57, no. 1, pp. 125-140, 2009. DOI: 10.2478/s11600-008-0070-6
25. Stozhkov, Y. I., N. S. Svirzhevsky, G. A. Bazilevskaya, M. B. Krainev, A. K. Svirzhevskaya, V. S. Makhmutov, V. I. Logachev, and E. V. Vashenyuk, Cosmic rays in the stratosphere in 2008–2010, Astrophys. Space Sci. Trans., 7, 379–382, 2011. www.astrophys-space-sci-trans.net/7/379/2011/doi:10.5194/astra-7-379-2011
26. Tomov, B., Dimitrov Pl., Matviichuk Yu., Dachev Ts., Galactic and Solar Cosmic Rays Study by Ground and Rocketborne Space Radiation Spectrometers-Dosimeters-Liulin-6R and Liulin-R, Proceedings of Fundamental Space Research Conference, 252-257, ISSBN 978-954-322-316-9, 2008. http://www.stil.bas.bg/FSR/PDF/TOP5Tomov_Borislav2242058.pdf